

Predicting rootzone soil moisture from surface observations in cropland using an exponential filter

Pedro Rossini | Andres Patrignani 

Dep. of Agronomy, Kansas State Univ.,
1712 Claflin Rd., 2004 Throckmorton Hall,
Manhattan, KS 66506, USA

Correspondence

Andres Patrignani, Dep. of Agronomy,
Kansas State Univ., 1712 Claflin Rd., 2004
Throckmorton Hall, Manhattan, KS 66506,
USA.

Email: andrespatrignani@ksu.edu

Assigned to Associate Editor Shannon
Osborne.

Abstract

Rootzone soil moisture provides valuable information to guide in-season management decisions in rainfed and irrigated agricultural systems. Measuring rootzone soil moisture usually requires the deployment of a vertical array of sensors, which can be costly and labor intensive. In this study, we tested the skill of an exponential filter to estimate rootzone soil moisture conditions from a time series of near-surface soil moisture observations. Daily soil moisture observations from a sensor at 10-cm depth were used to predict the soil water content at 30-, 50-, and 70-cm depth, and across the entire soil profile (0-to-80-cm depth) in four agricultural fields under irrigated and rainfed conditions. The characteristic time length was the only fitting parameter of the model, which was optimized for each site based on the Nash–Sutcliffe (NS) score. Across the four sites, the mean NS score at individual soil layers ranged from -0.64 to 0.73 , but the NS score at the profile level ranged between 0.29 and 0.84 . Predictions of soil water storage at the profile level based on near-surface soil moisture and the exponential filter resulted in average RMSE of 11 mm across the four locations. Our study shows that in agricultural fields the exponential filter performs better when considering the entire soil profile rather than individual soil layers.

1 | INTRODUCTION

Rootzone soil water storage is a decisive variable in irrigation scheduling (Hassanli et al., 2009; Irmak et al., 2012; Spencer et al., 2019) and a major factor controlling crop production in rainfed agricultural systems, particularly in semi-arid and subhumid areas (Falkenmark et al., 2001). Thus, accurate monitoring of rootzone soil moisture has the potential to reduce the amount of irrigation during the growing season, increase crop water use efficiency by improving the timing and amount of irrigation events, and increase crop yields or increase farm profits by making better in-season management decisions (Pereira, 2017). For instance, in corn (*Zea*

mays L.) fields located across Nebraska, soil moisture-based irrigation scheduling resulted in 33% less irrigation application relative to the farmer management practice (Irmak et al., 2012). Similarly, a multiyear study in the Mississippi River Valley found that irrigation scheduling based on soil moisture sensors was one of the key factors enabling a 39% reduction in irrigation water use while still allowing a grain yield increase of $\sim 3\%$ relative to yields using conventional irrigation practices in the region (Spencer et al., 2019).

A common practice to quantify rootzone soil water storage in agricultural fields is to use point-level soil moisture sensors based on electromagnetic principles. These types of sensors are one of the predominant soil moisture sensing technologies for both research-grade and consumer-grade sensors that typically offer relatively accurate ($\sim 0.03 \text{ m}^3 \text{ m}^{-3}$) measurements of soil water storage (Cosh et al., 2016), require

Abbreviations: EF, exponential filter; MBE, mean bias error; NS, Nash–Sutcliffe.

minimum sensor maintenance, and can be easily integrated with data logging and telemetry systems for near-real time soil moisture monitoring (Adla et al., 2020; Dobriyal et al., 2012). However, two important restrictions of traditional point-level sensors (i.e., two- and three-pronged sensors) are the reduced support volume (typically $<5,000\text{ cm}^3$) and the need for soil excavation or soil coring to install multiple sensors along the rootzone of common agricultural crops, which can become laborious and impractical for researchers and producers trying to represent areas of the field with different soils or topographic conditions. Even though new commercially available multi-depth soil moisture sensors have alleviated the laborious installation of traditional pronged sensors and can better represent profile dynamics with a single instrument, multi-depth sensors can be substantially more expensive and do not necessarily offer an advantage over pronged sensors in terms of better characterizing the field horizontal soil moisture spatial variability. However, with the advent of low-power wide-area networks and the development of more affordable soil moisture sensors, a cost-effective solution to increase the horizontal spatial coverage and reveal the spatiotemporal structure of soil moisture of agricultural fields could be achieved by deploying a spatially distributed wireless sensor network (Bogena et al., 2010). Because of the usually higher soil moisture spatial variability of shallow soil layers compared with deeper layers of the soil profile (Mahmood et al., 2012), field-scale wireless sensor networks could capture the most prominent changes in soil moisture conditions near the soil surface due to wetting and drying cycles and rely on a model to infer the soil moisture conditions at deeper soil layers.

Multiple filtering techniques have been successfully used to depth-scale surface soil moisture observations such as the exponential filter (EF) (Wagner et al., 1999), maximum entropy model (Al-Hamdan & Cruise, 2010), and wavelet analysis (Grinsted et al., 2004). In particular, the EF has received particular interest from the remote sensing community to estimate profile-level soil moisture conditions from shallow (i.e., 0–5 cm) measurements of soil water content from dedicated satellite missions such as the Soil Moisture and Ocean Salinity satellite (Ford et al., 2014). The EF is attractive because of the small number of parameters and the possibility to account for intermittently available surface soil moisture observations (Albergel et al., 2008; Mishra et al., 2020). For example, Ceballos et al. (2005) using the EF found a strong significant correlation ($r^2 = .75$) between rootzone (0-to-100-cm depth) soil moisture derived from European Remote Sensing Satellite scatterometer retrievals and in situ soil moisture observations in the Duero basin in Spain. Similarly, Peterson et al. (2016) working on a 25-ha grazing pasture in Canada concluded that the EF has the greatest potential to estimate rootzone soil moisture derived from near-surface soil moisture estimated from cosmic-ray neutron observations

Core Ideas

- An exponential filter was used to estimate rootzone soil moisture from near-surface sensors.
- The experiment was conducted in four agricultural fields under rainfed and irrigated conditions.
- Predictions with the exponential filter were most accurate at the profile level.
- The performance of the exponential filter seems to be affected by changes in crop sequence.

when compared with time-stable monitoring locations and representative landscape units. From the hydrological point of view, several studies have shown that rootzone soil moisture can be accurately predicted using near-surface (i.e., 5 and 10 cm) soil moisture observations using in situ soil moisture observations from mesoscale environmental monitoring networks (Ford et al., 2014; Wang et al., 2017).

Although substantial research has been reported using the EF to infer rootzone soil moisture from remote sensing soil moisture products and from in situ soil moisture observations in landscapes dominated by natural grassland vegetation, there is a gap in the scientific literature about using the EF to estimate rootzone soil moisture from near-surface in situ soil observations in agricultural production fields. We hypothesize that a single shallow soil moisture sensor coupled with the EF will result in rootzone soil moisture estimates that are comparable to a denser array of vertically installed sensors across the soil profile. The objective of this study was to investigate the accuracy of an EF coupled with daily in situ observations of surface soil moisture to estimate daily rootzone soil water storage.

2 | MATERIALS AND METHODS

2.1 | Sites and datasets

Soil moisture observations were collected in three different agricultural fields in central Kansas from October 2016 to September 2020 (Table 1). Site A is situated within the Kansas State University North Agronomy Farm Experiment Research Station near Manhattan, KS. The cropping system of Site A follows a no-till rotation based on winter wheat (*Triticum aestivum* L.), double crop soybean [*Glycine max* (L.) Merr.], and full season sorghum [*Sorghum bicolor* (L.) Moench] under rainfed conditions. Site B is situated near Hutchinson, KS, and the cropping system consists of a minimum tillage operation with a full season corn and soybeans rotation under a center pivot irrigation. Sites C and D

TABLE 1 Site, crop rotation, study period, and soil series and textural class for each soil horizon in the top 80 cm of the soil profile obtained from the USDA-NRCS Soil Survey Geodatabase

Site	Crop sequence ^a	Start date	End date	<i>N</i> d	Soil series	Horizon	Horizon depth cm	Textural class ^b
A	WW–F–SB	25 Oct. 2016	29 Oct. 2017	370	Kahola	Ap	0–20	Silt loam
						A	20–61	Silt loam
						AC	61–80	Silt loam
B	CN	22 June 2018	27 Aug. 2018	67	Avans	Ap	0–25	Sandy loam
						BA	25–36	Silt Loam
						Bt1	36–48	Clay Loam
						Bt2	48–76	Loam
C	CN–F–CN	26 Apr. 2019	18 Nov. 2020	573	Farnum	Ap	0–23	Loam
						Bt1	23–64	Loam
						Bt2	64–80	Sandy clay loam
D	CN–F	24 Apr. 2019	31 Mar. 2020	342	Crete	Ap	0–15	Silty clay loam
						BA	15–38	Silty clay loam
						Bt1	38–64	Silty clay
						Bt2	64–80	Silty clay

^aWW, winter wheat; SB, soybean; F, fallow; CN, corn.

^bSoil textural class for the top horizon in Sites B, C, and D was obtained from disturbed soil samples from the 0-to-15-cm layer and analyzed using the hydrometer method (Gavlak et al., 2003).

were both situated in an irrigated field with no-till crop rotation near Moundridge, KS, but each site was located in zones of the field with distinct soil type and topographic conditions. Site C was located at the bottom slope characterized by the Farnum series (fine-loamy, mixed, superactive, mesic Pachic Argiustolls) with loam soils (slopes 1–3%) with presence of fine gravel in the top soil horizons (Soil Survey Staff, 2020). Site D was located on the upland area of the field that is characterized by deep and moderately well drained Crete series (fine, smectitic, mesic Pachic Udertic Argiustolls) with silty clay loam soils and <1% slopes (Soil Survey Staff, 2020). Sites C and D were intentionally located in the same field following the results of a previous research study (Rossini et al., 2021) in the same field that subdivided the field into two distinct management zones based on soil moisture spatial variability. Time series ranged from a minimum of 66 d at Site B to a maximum of 572 d at Site C, spanning multiple phases of the crop rotation (Table 1). The region encompassing the three fields has an average annual rainfall of 800 mm, a mean annual temperature of 13 °C, and a mean minimum and maximum air temperature between –1 and 27 °C.

At each site, we deployed an in situ soil moisture monitoring station consisting of a datalogger (CR200X, Campbell Scientific) equipped with four soil water reflectometers (CS655, Campbell Scientific). The soil moisture sensors consist of two 12-cm-long stainless steel rods attached to an epoxy sensor head. All output variables from the sensor were collected at hourly intervals and were aggregated at daily intervals. All raw variables reported by the sensor were saved

including voltage ratio, relative permittivity, temperature, period average, and electrical conductivity. Electronic components were housed into an all-weather enclosure and the station was powered by a 10-W solar panel. For this study we assumed an 80-cm soil profile that was divided into four layers of 20 cm each. Sensors were installed by first creating a trench and then inserting each sensor horizontally into the undisturbed face of the trench at 10-, 30-, 50-, and 70-cm depth (Supplemental Figure S1). Each sensor depth is assumed to be located at the center of the layer that it represents (Cosh et al., 2021). For instance, the sensor deployed at 10-cm depth represents the soil water content of the 0-to-20-cm soil layer. The daily profile soil water storage was computed as follows:

$$S_t = \sum_{i=1}^4 (\theta_{it} z) \quad (1)$$

where S_t is the storage soil moisture (mm) on day t , the θ_{it} is the average volumetric water content of layer i on day t , and z is the thickness of the soil layers (mm), which in this study was constant with a value of 200 mm.

All sensor output variables, including soil temperature, dielectric permittivity, bulk electrical conductivity, and period average, were recorded at hourly intervals. A custom sensor calibration equation was developed under laboratory conditions using columns with packed soil from different parts of the fields. Known volumetric water content from the packed columns were used to fit a linear regression model as a

function of a linear model of the squared root of the dielectric permittivity measured by the sensor (Ledieu et al., 1986):

$$\theta = -0.0994 + 0.0968\sqrt{K_a} \quad (2)$$

where θ ($\text{m}^3 \text{m}^{-3}$) is the volumetric water content and K_a (unitless) is the real part of the apparent dielectric permittivity, and the two empirical parameters were obtained by optimization of the model based on ordinary least squares by using the *lsqcurvefit* function in Matlab 2018b (Mathworks). This calibration equation provided a RMSE of $0.028 \text{ cm}^3 \text{ cm}^{-3}$ on the calibration dataset with volumetric water contents ranging from 0.013 to $0.448 \text{ cm}^3 \text{ cm}^{-3}$. Although multiple studies have shown the pitfalls of using calibration equations developed using packed soil columns in laboratory conditions for field applications (Cosh et al., 2005; Logsdon, 2009; Ojo et al., 2015), our calibration improved the sensor accuracy for the soils in the calibration dataset compared with the factory default calibration that resulted in RMSE of $0.041 \text{ cm}^3 \text{ cm}^{-3}$. Since the surface soil moisture observations used as input in the EF were recorded with the same model of soil moisture sensors as in deeper layers of the soil profile, it is unlikely that a sensor bias was introduced in the validation of the filter, other than perhaps the need for a soil- and depth-specific sensor calibration that was not accounted for in our study. During the winter time, and a few times during the growing season, malfunctioning batteries and solar panels introduced some gaps in the temporal record. As a result, we only used soil moisture data for growing seasons and fallow periods with no missing observations. Soil moisture observations when the soil temperature was $<1^\circ \text{C}$ were removed due to changes in the dielectric permittivity of frozen soil water (Seyfried & Grant, 2007), and we replaced these values with a centered moving median filter (30-d window). A total of 7.5% of the daily soil moisture observations in the topmost sensor were replaced due to low temperatures in Site A and $<2.5\%$ in the topmost sensors of Sites C and D. No values were replaced due to the effect of low temperatures in Site B since the sensors were only deployed during the spring and summer seasons.

2.2 | Exponential filter description

The EF is a statistical filtering approach proposed by Wagner et al. (1999) and later reformulated in a recursive form by Albergel et al. (2008) with the aim of estimating rootzone soil moisture from surface soil moisture observations. This method simplifies the soil water balance using a two-layer approach, where the flux between these two layers is proportional to the difference in soil moisture content between the layers. The model assumes a constant pseudo-diffusivity factor that propagates fluctuations in surface soil moisture in

attenuated form to deeper soil layers. The recursive formulation to retrieve rootzone soil moisture from surface soil moisture observations can be expressed as

$$\text{SWI}_{m(n)} = \text{SWI}_{m(n-1)} + K_n [\text{ms}_{(n)} - \text{SWI}_{m(n-1)}] \quad (3)$$

where SWI_m is the soil water index in the rootzone, ms_n is the normalized soil moisture observed in the surface layer, n represent the time in days, and K is the gain function (range from 0 to 1) that is computed as

$$K_n = \frac{K_{n-1}}{K_{n-1} + e^{\frac{t_n - t_{n-1}}{T}}} \quad (4)$$

where $t_n - t_{n-1}$ is the difference in days between surface soil moisture observations (a value of 1 d in our study), and T is an empirical characteristic time length in days and the only unknown of the model. The parameter T is often assumed to represent soil hydraulic properties and the vertical anisotropy of the soil profile characterized by different soil texture and bulk density of the soil horizons that affect the temporal dynamics of soil moisture within the soil profile (Albergel et al., 2008; Ceballos et al., 2005). Therefore, the T parameter should be calibrated on each individual study site. To optimize the value of T parameter (T_{opt}), SWI_m was computed using different values of T (1–60 d) (Wang et al., 2017). The Nash–Sutcliffe (NS) score (Nash & Sutcliffe, 1970) was used to evaluate the performance of the EF (Albergel et al., 2008; Ford et al., 2014; Wang et al., 2017). The NS score can range from $-\infty$ to 1, where a value of 1 corresponds to a perfect match between predicted and observed data, whereas values lower than 0 typically represent that the observed mean is a better predictor than the approximation made using the EF. To better evaluate the performance of the EF we also computed the Pearson correlation coefficient (r), RMSE, and mean bias error (MBE). To obtain $\text{ms}_{n'}$, the observed volumetric water content at 10-cm depth was normalized in the range 0 to 1 using the *normalize* function with the *range* normalization method in Matlab. Daily observations of rootzone soil moisture were also normalized to obtain the observed soil water index $\text{SWI}_{(\text{obs})}$. For initialization of the EF we assumed that $\text{SWI}_{m(1)} = \text{ms}_{(1)}$ and $K_1 = 1$ (Albergel et al., 2008).

3 | RESULTS AND DISCUSSION

Near-surface (i.e., 10-cm depth) soil moisture observations were coupled with an EF to estimate soil water dynamics at individual soil depths (i.e., 30, 50, and 70 cm; Figure 1) and at the profile level (i.e. 0–80 cm; Figure 2) at four different sites across central Kansas from October 2016 to March 2020 (Table 1). Based on the NS score, the EF resulted in more accurate predictions of soil water dynamics when

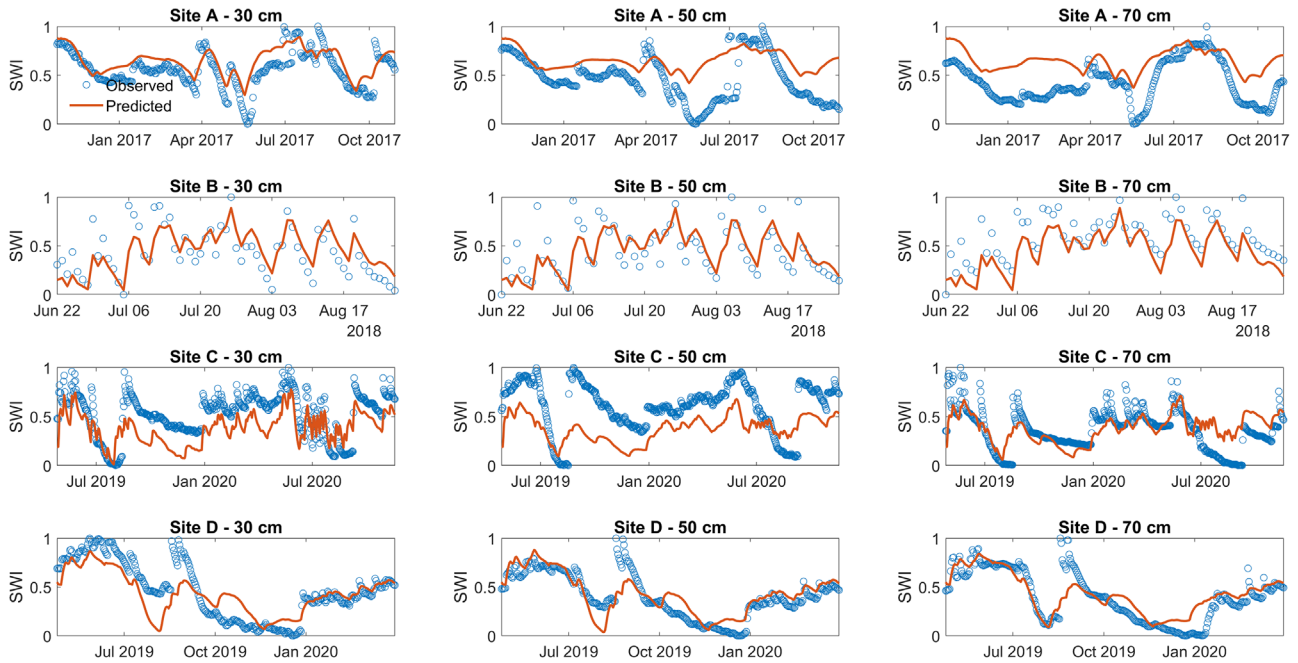


FIGURE 1 Observed (blue open circles) and predicted (red solid line) soil water index (SWI, unitless) at 30- 50-, and 70-cm depth for the four study sites in central Kansas. Predictions were generated by combining soil moisture observations from a sensor at 10-cm depth and the exponential filter

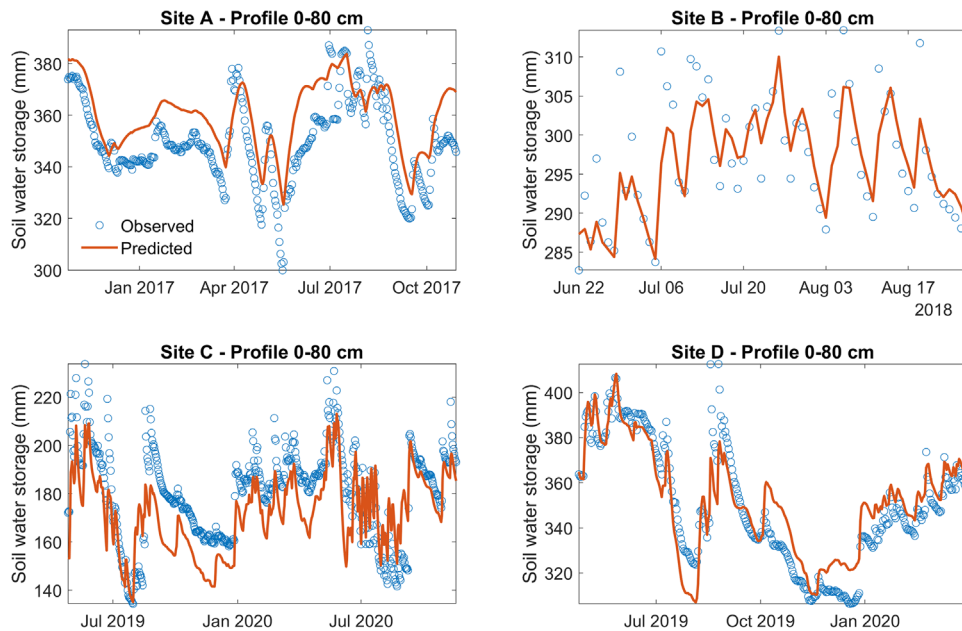


FIGURE 2 Observed (blue open circles) and predicted (red solid line) soil water storage (mm) for Sites A, B, C, and D in the 0-to-80-cm soil layer solely using soil moisture information from a sensor at 10-cm depth and the exponential filter

considering the soil moisture dynamics across the entire soil profile compared with individual soil layers (Table 2). Across all four sites, the mean NS score at individual soil layers ranged from -0.64 to 0.73 , whereas the NS score at the profile level was generally higher and more consistent than individual soil layers with NS scores ranging from 0.29 in Site A to 0.84

in Site D (Table 2). The trend in the NS scores was closely followed by the trend in RMSE and MBE error metrics. For instance, the 50- and 70-cm soil depths in Site A, and the 50-cm depth in Site C that resulted in negative NS scores, also resulted in the three largest RMSE values and the three largest MBE magnitudes, showing that individual soil layers in the

TABLE 2 Optimized characteristic time length parameter (T_{opt}) for each site depth, Nash–Sutcliffe score (NS), Pearson correlation coefficient (r), mean bias error (MBE), and rRMSE of the normalized soil water index and the actual soil water storage

Site	Depth	T_{opt}	NS	r	MBE	RMSE	RMSE
	cm	d					mm
A	30	12	0.45	.83	−0.09	0.14	2.9
	50	26	−0.23	.68	−0.18	0.25	5.1
	70	18	−0.64	.77	−0.23	0.27	5
	Profile	10	0.29	.84	−0.11	0.15	13.6
B	30	1	0.62	.79	−0.01	0.15	0.9
	50	1	0.57	.76	0.01	0.16	2.3
	70	1	0.31	.89	0.14	0.17	1.8
	Profile	1	0.7	.85	0.02	0.14	4.3
C	30	3	0.13	.73	0.14	0.21	5.4
	50	11	−0.45	.64	0.23	0.30	5.9
	70	7	0.36	.61	−0.02	0.16	4.6
	Profile	2	0.47	.8	0.08	0.14	14.1
D	30	6	0.66	.83	0.03	0.17	4.5
	50	6	0.70	.85	−0.02	0.12	3.6
	70	9	0.73	.87	−0.03	0.13	2.9
	Profile	2	0.84	.92	−0.02	0.10	10.8

middle of the soil profile show a weaker coupling with near-surface observations compared with considering the entire soil profile. An incomplete picture of the relationship between near-surface and deeper soil layers could be reached by solely looking at the Pearson correlation coefficient, which only captures the degree of linear association between two variables. For instance, from our analysis, r values were $>.7$ in 13 out of the 16 tested soil depths, highlighting the strong positive linear relationship between near-surface and deeper soil moisture conditions (Table 2), but this view offers little information about systematic biases in model predictions. The prediction in the 70-cm soil layer at Site A is a great example of how the coefficient of correlation ($r = .77$) masks a large prediction bias in the EF model (NS = -0.64) as a consequence of decoupled conditions between near-surface and subsurface soil moisture conditions (Figure 1). This discrepancy may be caused by soil layers with different soil texture or due to the presence of an actively growing vegetation (Calvet & Noilhan, 2000); in our case, an actively growing vegetation likely had a stronger impact since the soil horizons of Site A have similar soil textural classes, although soil hydraulic differences can still exist between horizons. Different patterns in soil texture and soil moisture content can also influence crop root distribution and root activity, further contributing to decoupled dynamics between surface conditions and rootzone conditions. Our results agree well with those of Ford et al. (2014), who conclude that the EF has a diminished accuracy in soil with heterogeneous properties and during times of soil moisture recharge and utilization.

Further inspection of model errors across different phases of the crop rotation revealed that low errors between predicted and observed SWI were mainly associated with fallow periods (e.g., Sites C and D) that often promote profile soil water recharge. Soil moisture recharge periods increase the coupling strength between surface observations and deeper soil layers (Mahmood et al., 2012), increasing the prediction accuracy of the EF (Ford et al., 2014). On the other hand, during periods of active crop growth, the predicted profile SWI showed the largest errors (e.g., Sites A and C at 50-cm depth). A potential source of error could be attributed to the transient patterns of root water uptake in intermediate soil layers that may not be captured by the sensor near the soil surface and by a single fitting parameter in the EF model that represents both the growing season and the fallow season coupling between near-surface and deeper soil layers. For instance, Sites A and C spanned two growing seasons with a fallow period between the growing seasons that likely affected the ability of the EF to capture the fluctuations in soil moisture conditions with only one degree of freedom (i.e., parameter T). In Site A, this lack of agreement between observed and predicted soil moisture could also be attributed to the presence of winter wheat and soybeans that likely resulted in a differential root water uptake that may not have been evident in the near-surface soil moisture dynamics, hence the difference was not captured by the EF. Consequently, NS scores values at Site A in 50- and 70-cm layers reached negative NS scores of -0.23 and -0.64 (Table 2), meaning that the average soil moisture was a better predictor than the model. This limitation at 50 cm could be

attributed to active root water uptake coupled with temporal delays for soil moisture redistribution between the soil surface and the deeper layers of the soil profile (Weaver & Darland, 1949). Negative NS scores at intermediate soil depths have also been reported by Wang et al. (2017) under grassland vegetation across stations of the Soil Climate Analysis Network. On the contrary, Sites B and D spanned periods with a single crop and had higher average NS scores of 0.39 and 0.79, respectively.

Our results suggest that the EF may fail to capture changes in the rootzone soil moisture related to changes in the land cover. This deficiency could be attributed to the fact that surface soil moisture dynamics at 10-cm depth and the rootzone soil moisture dynamics in the 20-to-80-cm depth followed different patterns of root water uptake along the different phases of the crop rotation, which can directly affect the performance of the filter (Albergel et al., 2008; Ford et al., 2014; Wang et al., 2017). To improve model performance, a time-dependent T parameter may allow the EF model to better account for the transient patterns in root water uptake across the soil profile. Previous studies using the EF have primarily involved in situ soil moisture observations from sparse networks under natural grassland vegetation, which likely exhibit a more stable relationship between near-surface and subsurface soil moisture dynamics than agricultural fields with changing crops and fallow periods. Under natural grassland conditions, a single calibrated T parameter seems to capture the soil hydraulic properties and the seasonal changes in vegetation, while in agricultural fields the different phases of the crop rotation and the associated soil water extraction patterns seem to affect the ability of the EF to predict rootzone soil moisture dynamics in terms of the NS score. The parameter T was optimized for each site based on the highest NS score (Table 2). Average values of T_{opt} ranged from 1 d in Site B to 26 d in Site A, with a clear variation across sites and depths matching previous findings by (Albergel et al., 2008). Smaller values of T_{opt} were observed in Site B, which is likely attributed to the presence of sandy loam soils with large hydraulic conductivity and low water holding capacity, thus enabling a rapid soil water redistribution across the soil profile. Similar findings have been observed by Wang et al. (2017) while working with in situ soil moisture information from the Nebraska Mesonet, in which the magnitude of T_{opt} was negatively correlated to sand fraction.

In terms of millimeters of soil water storage, predictions at individual soil layers (i.e., 30, 50, and 70-cm depth) based on near-surface soil moisture resulted in ≤ 5 mm in 9 out of the 12 soil depths across all sites and between 4.3 mm (Site B) and 14.1 mm (Site C) when considering the entire profile (Table 2, Figure 2). Considering the average RMSE of 11 mm at the profile level across the four study sites, using near-surface surface soil moisture sensors coupled with the EF seems a

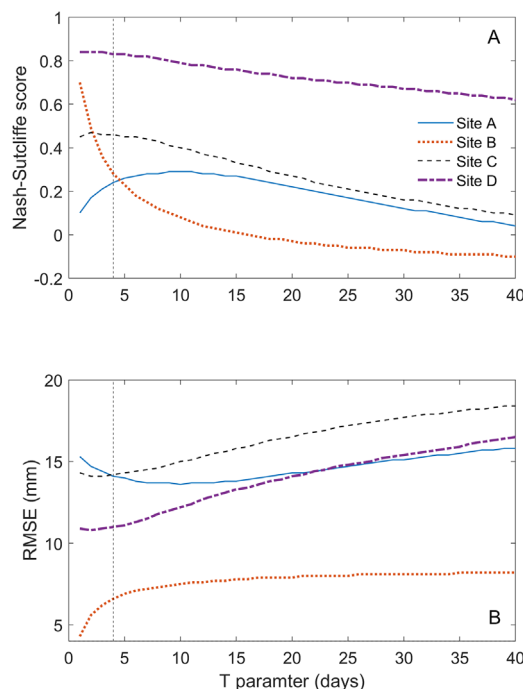


FIGURE 3 Sensitivity analysis of the Nash–Sutcliffe score and the RMSE in terms of soil water storage for the entire soil profile (0–80 cm) for a range of characteristic time length T . Vertical dashed line denotes the average of optimized T (T_{opt}) at the profile level for all sites

suitable alternative for guiding irrigation scheduling, but more research is required in cropland environments to better understand the impact of soil layering and the vertical patterns in root water uptake on the parameters of the EF during the different phases of the crop rotation.

In order to assess the sensitivity of the NS score and the RMSE in the predicted soil water storage as a function of the characteristic time length parameter T , we conducted a simple sensitivity analysis by ranging T from 1 to 40 d only using data at the profile level (0–80 cm; Figure 3). Overall, the NS tended to decrease with increasing T values in all four sites, particularly in the range of 10–40 d. At the profile level, the NS score was most sensitive to T at Site B, which is characterized by sandy loam soils that can exhibit rapid changes in soil moisture conditions within a short period of time. In fact, the rapid decrease in the NS score with increasing values of T suggests that for Site B the T_{opt} could have been even lower than a single day if we had considered hourly time steps in our analysis. As expected, the error in the predicted profile level soil water storage increased with increasing characteristic time length. However, the RMSE in the predicted soil water storage was rather insensitive to the characteristic time length, with Site D exhibiting the largest fluctuation of ~ 5 mm between $T = 2$ d and $T = 40$ d. Using the average of T_{opt} (i.e., $T = 4$ d) as a single value for the entire study period would have resulted in $\text{RMSE} < 15$ mm for all sites, which is

encouraging considering the range of soil textural classes and crop sequences in our study.

4 | CONCLUSION

The proposed method of estimating rootzone soil moisture by only deploying a near-surface sensor coupled with an EF presents clear practical advantages over excavating and deploying multiple sensors along the soil profile of large agricultural fields. Predictions using the EF resulted most accurate when considering the full soil profile (i.e., 0-to-80-cm depth), followed by predictions at depths immediately below the sensor at 10-cm depth (i.e., 30-cm layer). The timing and vertical distribution of root water uptake due to actively growing crops likely caused a decoupling between surface and subsurface soil water dynamics that was not captured by the EF model using a single time characteristic length parameter. Future studies using the EF in agricultural fields conditions should explore the separate effect of soil hydraulic properties and crop sequence. One improvement in the EF that could better capture the effects of crop sequence is the implementation of a time-dependent characteristic time length parameter. Another possible alternative would be to decouple the soil hydraulic and crop sequence effects using two constant and independent T parameters combined in the computation of the gain function (Equation 4). Modifications of this type would require supporting evidence and validation with in situ soil moisture observations along the rootzone of agricultural crops obtained via soil sampling, dense profile sensor arrays, or multi-depth sensors, and would also require caution to preserve the level of parsimony of the filter. However, the sensitivity analysis revealed that at the profile level the NS score tends to be more sensitive than the RMSE in predicted soil water storage, which provides supporting evidence that the decision of using a constant T parameter across multiple soils and crop sequences may be sufficient for some agricultural applications. Overall, the EF showed promising potential to extend near-surface soil moisture conditions to estimate profile-level soil water storage in cropland fields that can be used for guiding in-season management decisions and irrigation scheduling.

ACKNOWLEDGMENTS

The authors would like to thank Ray and Ryan Flickner from the Flickner Innovation Farm, Brian Yutzy from Southwest Seeds, and Dr. Kraig Roozeboom for allowing us to collect soil moisture observations for this project. This project was supported by the Kansas Corn Commission Awards KCC1915 and KCC2007, National Science Foundation (NSF) Established Program to Stimulate Competitive Research (EPSCoR) Award 1001140, and the Kansas State University Agricultural Experiment Station (Contribution 22-038-J).

AUTHOR CONTRIBUTIONS

Pedro Rossini: Conceptualization; Data curation; Formal analysis; Investigation; Methodology; Visualization; Writing-original draft; Writing-review & editing. Andres Patrignani: Investigation; Project administration; Supervision; Writing-review & editing.

CONFLICT OF INTEREST

The authors declare no conflict of interest.

ORCID

Andres Patrignani  <https://orcid.org/0000-0001-5955-5877>

REFERENCES

- Adla, S., Rai, N. K., Karumanchi, S. H., Tripathi, S., Disse, M., & Pande, S. (2020). Laboratory calibration and performance evaluation of low-cost capacitive and very low-cost resistive soil moisture sensors. *Sensors*, 20(2), 363. <https://doi.org/10.3390/s20020363>
- Al-Hamdan, O. Z., & Cruise, J. F. (2010). Soil moisture profile development from surface observations by principle of maximum entropy. *Journal of Hydrologic Engineering*, 15(5), 327–337. [https://doi.org/10.1061/\(asce\)he.1943-5584.0000196](https://doi.org/10.1061/(asce)he.1943-5584.0000196)
- Albergel, C., Rüdiger, C., Pellarin, T., Calvet, J.-C., Fritz, N., Froissard, F., Suquia, D., Petitpa, A., Pignat, B., & Martin, E. (2008). From near-surface to root-zone soil moisture using an exponential filter: An assessment of the method based on in-situ observations and model simulations. *Hydrology and Earth System Sciences*, 12, 1323–1337. <https://doi.org/10.5194/hess-12-1323-2008>
- Allen, R. G., Pereira, L. S., Raes, D., & Smith, M. (1998). *Crop evapotranspiration: Guidelines for computing crop water requirements* (Irrigation and Drainage Paper 56). FAO.
- Bogena, H. R., Herbst, M., Huisman, J. A., Rosenbaum, U., Weuthen, A., & Vereecken, H. (2010). Potential of wireless sensor networks for measuring soil water content variability. *Vadose Zone Journal*, 9(4), 1002–1013. <https://doi.org/10.2136/vzj2009.0173>
- Calvet, J. C., & Noilhan, J. (2000). From near-surface to root-zone soil moisture using year-round data. *Journal of Hydrometeorology*, 1(5), 393–411. [https://doi.org/10.1175/1525-7541\(2000\)001<0393:FNSTRZ>2.0.CO;2](https://doi.org/10.1175/1525-7541(2000)001<0393:FNSTRZ>2.0.CO;2)
- Ceballos, A., Scipal, K., Wagner, W., & Martínez-Fernández, J. (2005). Validation of ERS scatterometer-derived soil moisture data in the central part of the Duero Basin, Spain. *Hydrological Processes*, 19(8), 1549–1566. <https://doi.org/10.1002/hyp.5585>
- Cosh, M. H., Caldwell, T. G., Baker, C. B., Bolten, J. D., Edwards, N., Goble, P., Hofman, H., Ochsner, T. E., Quiring, S., Schalk, C., & Skumanich, M., (2021). Developing a strategy for the National Coordinated Soil Moisture Monitoring Network. *Vadose Zone Journal*, 20(4), e20139. <https://doi.org/10.1002/vzj2.20139>
- Cosh, M. H., Jackson, T. J., Bindlish, R., Famiglietti, J. S., & Ryu, D. (2005). Calibration of an impedance probe for estimation of surface soil water content over large regions. *Journal of Hydrology*, 311(1–4), 49–58. <https://doi.org/10.1016/j.jhydrol.2005.01.003>
- Cosh, M. H., Ochsner, T. E., Mckee, L., Dong, J., Basara, J. B., Evett, S. R., Hatch, C. E., Small, E. E., Steele-Dunne, S. C., Zreda, M., & Sayde, C. (2016). The soil moisture active passive Marena, Oklahoma, in situ sensor testbed (SMAP-MOISST): Testbed design and

- evaluation of in situ sensors. *Vadose Zone Journal*, 15(4), <https://doi.org/10.2136/vzj2015.09.0122>
- Dobriyal, P., Qureshi, A., Badola, R., & Hussain, S. A. (2012). A review of the methods available for estimating soil moisture and its implications for water resource management. *Journal of Hydrology*, 458–459, 110–117. <https://doi.org/10.1016/j.jhydrol.2012.06.021>
- Falkenmark, M., Fox, P., Persson, G., & Rockström, J. (2001). *Water harvesting for upgrading of rainfed agriculture: Problem analysis and research needs*. Stockholm International Water Institute.
- Ford, T. W., Harris, E., & Quiring, S. M. (2014). Estimating root zone soil moisture using near-surface observations from SMOS. *Hydrology and Earth System Sciences*, 18(1), 139–154. <https://doi.org/10.5194/hess-18-139-2014>
- Gavlak, R., Horneck, D., Miller, R. O., & Kotuby-Amacher, J. (2003). *Soil, plant and water reference methods for the western region* (WCC-103 Publication). Colorado State University.
- Grinsted, A., Moore, J. C., & Jevrejeva, S. (2004). Application of the cross wavelet transform and wavelet coherence to geophysical time series. *Nonlinear Processes in Geophysics*, 11(5/6), 561–566. <https://doi.org/10.5194/npg-11-561-2004>
- Hassanli, A. M., Ebrahimizadeh, M. A., & Beecham, S. (2009). The effects of irrigation methods with effluent and irrigation scheduling on water use efficiency and corn yields in an arid region. *Agricultural Water Management*, 96(1), 93–99.
- Irmak, S., Burgert, M. J., Yang, H. S., Cassman, K. G., Walters, D. T., Rathje, W. R., Payero, J. O., Grassini, P., Kuzila, M. S., Brunkhorst, K. J., Eisenhauer, D. E., Kranz, W. L., Vandewalle, B., Rees, J. M., Zoubek, G. L., Shapiro, C. A., & Teichmeier, G. J. (2012). Large-scale on-farm implementation of soil moisture-based irrigation management strategies for increasing maize water productivity. *Transactions of the ASABE*, 55(3), 881–894. <https://doi.org/10.13031/2013.41521>
- Ledieu, J., De Ridder, P., De Clerck, P., & Dautrebande, S. (1986). A method of measuring soil moisture by time-domain reflectometry. *Journal of Hydrology*, 88(3–4), 319–328. [https://doi.org/10.1016/0022-1694\(86\)90097-1](https://doi.org/10.1016/0022-1694(86)90097-1)
- Logsdon, S. D. (2009). CS616 calibration: Field versus laboratory. *Soil Science Society of America Journal*, 73(1), 1–6. <https://doi.org/10.2136/sssaj2008.0146>
- Mahmood, R., Littell, A., Hubbard, K. G., & You, J. (2012). Observed data-based assessment of relationships among soil moisture at various depths, precipitation, and temperature. *Applied Geography*, 34, 255–264. <https://doi.org/10.1016/j.apgeog.2011.11.009>
- Mishra, V., Ellenburg, W. L., Markert, K. N., & Limaye, A. S. (2020). Performance evaluation of soil moisture profile estimation through entropy-based and exponential filter models. *Hydrological Sciences Journal*, 65(6), 1036–1048. <https://doi.org/10.1080/02626667.2020.1730846>
- Nash, J. E., & Sutcliffe, J. V. (1970). River flow forecasting through conceptual models part I: A discussion of principles. *Journal of Hydrology*, 10(3), 282–290. [https://doi.org/10.1016/0022-1694\(70\)90255-6](https://doi.org/10.1016/0022-1694(70)90255-6)
- Ojo, E. R., Bullock, P. R., L'heureux, J., Powers, J., McNairn, H., & Pacheco, A. (2015). Calibration and evaluation of a frequency domain reflectometry sensor for real-time soil moisture monitoring. *Vadose Zone Journal*, 14(3). <https://doi.org/10.2136/vzj2014.08.0114>
- Pereira, L. S. (2017). Agriculture and food: Challenges and issues. *Water Resources Management*, 31(10), 2985–2999. <https://doi.org/10.1007/s11269-017-1664-z>
- Peterson, A. M., Helgason, W. D., & Ireson, A. M. (2016). Estimating field-scale root zone soil moisture using the cosmic-ray neutron probe. *Hydrology and Earth System Sciences*, 20(4), 1373–1385. <https://doi.org/10.5194/hess-20-1373-2016>
- Rossini, P. R., Ciampitti, I. A., Hefley, T., & Patrignani, A. (2021). A soil moisture-based framework for guiding the number and location of soil moisture sensors in agricultural fields. *Vadose Zone Journal*, <https://doi.org/10.1002/vzj2.20159> (in press).
- Seyfried, M. S., & Grant, L. E. (2007). Temperature effects on soil dielectric properties measured at 50 MHz. *Vadose Zone Journal*, 6(4), 759–765. <https://doi.org/10.2136/vzj2006.0188>
- Soil Survey Staff. (2020). *Web soil survey*. USDA-NRCS. <https://websoilsurvey.sc.egov.usda.gov/>
- Spencer, G. D., Krutz, L. J., Falconer, L. L., Henry, W. B., Henry, C. G., Larson, E. J., Pringle III, H. C., Bryant, C. J., & Atwill, R. L. (2019). Irrigation water management technologies for furrow-irrigated corn that decrease water use and improve yield and on-farm profitability. *Crop, Forage & Turfgrass Management*, 5(1), 180100. <https://doi.org/10.2134/cftm2018.12.0100>
- Wagner, W., Lemoine, G., & Rott, H. (1999). A method for estimating soil moisture from ERS scatterometer and soil data. *Remote Sensing of Environment*, 70(2), 191–207. [https://doi.org/10.1016/S0034-4257\(99\)00036-X](https://doi.org/10.1016/S0034-4257(99)00036-X)
- Wang, T., Franz, T. E., You, J., Shulski, M. D., & Ray, C. (2017). Evaluating controls of soil properties and climatic conditions on the use of an exponential filter for converting near surface to root zone soil moisture contents. *Journal of Hydrology*, 548, 683–696. <https://doi.org/10.1016/j.jhydrol.2017.03.055>
- Weaver, J. E., & Darland, R. W. (1949). Soil-root relationships of certain native grasses in various soil types. *Ecological Monographs*, 19(4), 303–338. <https://doi.org/10.2307/1943273>

SUPPORTING INFORMATION

Additional supporting information may be found in the online version of the article at the publisher's website.

How to cite this article: Rossini, P., & Patrignani, A. Predicting rootzone soil moisture from surface observations in cropland using an exponential filter. *Soil Sci Soc Am J*, 2021;1–9. <https://doi.org/10.1002/saj2.20319>